

# Quantum rotational band model for the Heisenberg molecular magnet $\{\text{Mo}_{72}\text{Fe}_{30}\}$

JÜRGEN SCHNACK<sup>1</sup>, MARSHALL LUBAN<sup>2</sup>, and ROBERT MODLER<sup>2</sup>

<sup>1</sup> *Universität Osnabrück, Fachbereich Physik, D-49069 Osnabrück, Germany*

<sup>2</sup> *Ames Laboratory & Department of Physics and Astronomy, Iowa State University, Ames, Iowa 50011, USA*

PACS. 75.10.Jm – Quantized spin models.

PACS. 75.50.Xx – Molecular magnets.

**Abstract.** – We derive the low temperature properties of the molecular magnet  $\{\text{Mo}_{72}\text{Fe}_{30}\}$ , where 30  $\text{Fe}^{3+}$  paramagnetic ions occupy the sites of an icosidodecahedron and interact via isotropic nearest-neighbour antiferromagnetic Heisenberg exchange. The key idea of our model (J.S. & M.L.) is that the low-lying excitations form a sequence of “rotational bands”, i.e., for each such band the excitation energies depend quadratically on the total spin quantum number. For temperatures below 50 mK we predict that the magnetisation is described by a staircase with 75 equidistant steps as the magnetic field is increased up to a critical value and saturated for higher fields. For higher temperatures thermal broadening effects wash out the staircase and yield a linear ramp below the critical field, and this has been confirmed by our measurements (R.M.). We demonstrate that the lowest two rotational bands are separated by an energy gap of 0.7 meV, and this could be tested by EPR and inelastic neutron scattering measurements. We also predict the occurrence of resonances at temperatures below 0.1 K in the proton NMR spin-lattice relaxation rate associated with level crossings. As rotational bands characterize the spectra of many magnetic molecules our method opens a new road towards a description of their low-temperature behaviour which is not otherwise accessible.

*Introduction.* – A new class of magnetic compounds known as molecular magnets [1] is attracting much attention. These compounds can be synthesized as single crystals of identical molecular units, each containing several paramagnetic ions that mutually interact via Heisenberg exchange. The intermolecular magnetic interactions are in the great majority of cases utterly negligible as compared to intramolecular magnetic interactions. Measurements of the magnetic properties therefore reflect those of the common, individual molecular unit. Molecular magnets such as  $\{\text{Mn}_{12}\}$  and  $\{\text{Fe}_8\}$  have been the focal point for intense study of subjects of broad scientific importance, such as quantum tunneling of magnetisation and quantum coherence [2]. However, it is doubtful [3] that larger symmetric arrays of paramagnetic ions can be accommodated in such polynuclear coordination complexes utilizing simple organic bridging ligands. Very recently the first examples of a new paradigm of molecular magnets, based on so-called Keplerate structures, have been synthesized [4], and these offer numerous avenues for obtaining truly giant, highly symmetric arrays of paramagnetic ions.

The archetype of this new class is referred to as  $\{\text{Mo}_{72}\text{Fe}_{30}\}$  [4]. Embedded within a (diamagnetic) host molecule (mol. wt. 18,649), 30  $\text{Fe}^{3+}$  paramagnetic ions (spins  $s = 5/2$ ) occupy the sites of an icosidodecahedron and interact via isotropic, nearest-neighbour antiferromagnetic exchange. This Keplerate and its interlinked derivatives [5] pose a major theoretical challenge. The dimension of the Hilbert space for  $\{\text{Mo}_{72}\text{Fe}_{30}\}$  is a staggering  $6^{30}$ , precluding the calculation of the energy eigenvalues on any computer.

In this Letter we show that despite this immense obstacle the major low-temperature properties of  $\{\text{Mo}_{72}\text{Fe}_{30}\}$  can be calculated. Rather than pursue the futile task of diagonalizing the Heisenberg Hamiltonian [see (1)], we adopt an approximate, diagonalizable Hamilton operator [see (4)] which properly incorporates the generic result that the low-lying magnetic energy levels of a wide class of molecular magnets are arranged as parallel rotational bands. These rotational bands reflect the underlying sublattice structure of the spin array [6, 7] that has been found for the corresponding classical system [8]. But in contrast to the classical model and approximations like high-temperature series expansions the present approach enables us to access the properties of giant magnetic molecules for very low temperatures. We are also able to show that the predictions of the classical model extend to temperatures as low as 100 mK with very good accuracy for the special case of  $\{\text{Mo}_{72}\text{Fe}_{30}\}$ . In particular, we present our theoretical predictions for the temperature and field dependence of the magnetisation, and for the resonances of the spin-lattice relaxation rate of  $\{\text{Mo}_{72}\text{Fe}_{30}\}$ . We also show that our experimental findings directly reflect the existence of rotational bands.

*Rotational band Hamiltonian.* – The Hamiltonian for the isotropic Heisenberg model including the interaction with an external magnetic field  $B$  reads

$$\tilde{H} = -2J \sum_{(u,v)} \tilde{\mathbf{S}}(u) \cdot \tilde{\mathbf{S}}(v) + g\mu_B B \tilde{S}_z, \quad (1)$$

where  $J$  is the exchange constant with units of energy, and  $J < 0$  corresponds to antiferromagnetic coupling,  $g$  is the spectroscopic splitting factor, and  $\mu_B$  is the Bohr magneton. The vector operators  $\tilde{\mathbf{S}}(u)$  are the spin operators (in units of  $\hbar$ ) of the individual paramagnetic ions with spin  $s$ . The sum in (1) runs over all distinct nearest-neighbour pairs  $(u, v)$  of spins of a single molecule at positions  $u$  and  $v$ . Since the Hamiltonian commutes with the operators  $\tilde{\mathbf{S}}^2$  and  $\tilde{S}_z$  of the total spin, the eigenstates of  $\tilde{H}$  may be classified using the quantum numbers  $S$  and  $M$ .

In order to develop an approximate quantum model of  $\{\text{Mo}_{72}\text{Fe}_{30}\}$ , we first exploit the fact that the set of minimal energies for each  $S$  forms a rotational band,

$$E_{S,min} \approx -J[D(N, s)/N]S(S+1) + E_a. \quad (2)$$

This has been noted on several occasions for ring structures with an even number  $N$  of sites [9, 10]. Elsewhere we reported that all finite Heisenberg systems with isotropic and homogeneous antiferromagnetic exchange (including rings for both even and odd  $N$ , tetrahedron, cube, octahedron, icosahedron, triangular prism, and axially truncated icosahedron) exhibit a rotational band [6]. For high-symmetry systems we provided an expression for the classical limit  $D(N, \infty)$ , henceforth denoted by  $D$ , which yields  $D = 4$  for rings with even  $N$ , see also [10], and  $D = 6$  for the icosidodecahedron, cube, and octahedron. Our investigations [6] have shown that the numerical value of  $D(N, s)$  for any finite  $s$  is always a little larger than  $D$ . This difference can be taken as a measure of quantum spin effects; consistently it is largest for  $s = 1/2$ .

The constant offset  $E_a$  in (2) is to be selected so that the highest level of the rotational band, which occurs for  $S = Ns$ , agrees with the largest energy eigenvalue of (1). The corresponding eigenvector is the ground state eigenvector for the counterpart ferromagnetic system. Thus the largest energy eigenvalue serves as an anchor in all approximations of the rotational band [6]. Summarizing, for the molecular magnet  $\{\text{Mo}_{72}\text{Fe}_{30}\}$  the lowest rotational band is given by

$$E_{S,\min} = -\frac{J}{5} S(S+1) + 60Js \left( s + \frac{1}{10} \right) . \quad (3)$$

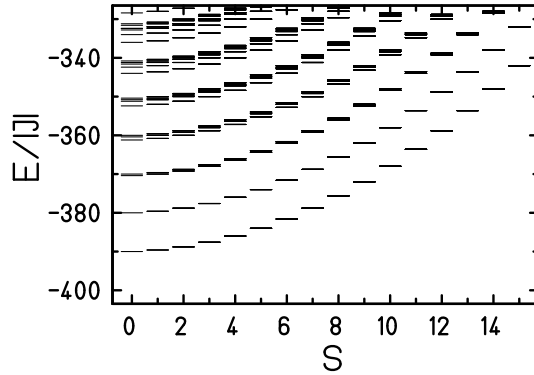


Fig. 1 – Low-lying energy eigenvalues using the approximate Hamiltonian (4) with  $B = 0$ . The levels of the lowest band are given by (3).

The rotational band (3) by itself is insufficient for calculating observables at low temperatures; it is essential to include the other low-lying excitation energies. This can be achieved via the introduction of an effective Hamiltonian whose form is set by incorporating the known symmetry of the spin array (icosidodecahedron), which is similar to that of the triangular lattice. Therefore, the low-lying spectrum can be understood as originating from three interacting sublattice spins [7]. These findings are supported by the fact that also the exact classical ground state of the icosidodecahedron for  $J < 0$  is describable in terms of three sublattice spin vectors  $\vec{S}_A$ ,  $\vec{S}_B$ , and  $\vec{S}_C$  with  $S_A = S_B = S_C = 25$ , and with relative angles of  $120^\circ$  [8]. We thus adopt as our effective Hamiltonian, replacing the field-free term of (1), see also [6, 7, 11],

$$\tilde{H}_1^{\text{eff}} = -\frac{J}{5} [\tilde{S}^2 - (\tilde{S}_A^2 + \tilde{S}_B^2 + \tilde{S}_C^2)] . \quad (4)$$

The three sublattice spin quantum numbers,  $S_A, S_B, S_C$ , can assume values  $0, 1, \dots, 25$ . The sublattice spin operators mutually commute and they also commute with  $\tilde{H}_1^{\text{eff}}$ . Thus the eigenvalues of  $\tilde{H}_1^{\text{eff}}$  are given in terms of the quantum numbers  $S, S_A, S_B$ , and  $S_C$ . The lowest rotational band, (3), arises upon choosing  $S_A = S_B = S_C = 25$  and allowing  $S$  to extend from 0 to 75. The next higher rotational band, see Fig. 1, is obtained for the choice  $S_A = S_B = 25, S_C = 24$  and its permutations. Note that these two bands are separated by an energy gap  $\Delta = 10J$ . Continuing this process leads to a sequence of parabolic bands. This is rather realistic for the second band, and indeed observed in many finite Heisenberg systems, compare Figs. 1, 3, and 4 in [6].

*Experimental implications.* – The theoretical result for  $\mathcal{M}/(g\mu_B)$  versus  $B$  at  $T = 0$  K, as obtained using (4) and a Zeeman term, is a staircase with 75 steps of unit height which terminates at the critical field  $B_c = 30|J|/(g\mu_B) = 17.7$  T. The values of  $J$  and  $g$  have been determined by high-temperature, low-field magnetic susceptibility measurements [12]:  $J/k_B = -0.783$  K, and  $g = 1.974$ . For  $B > B_c$  all spins are aligned parallel and the total moment is given by  $\mathcal{M} = 75g\mu_B$ .

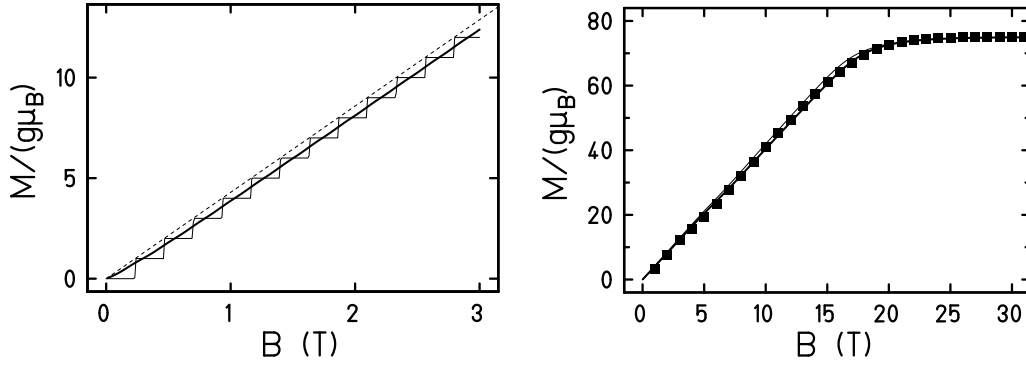


Fig. 2 – L.h.s.: The magnetisation according to (4) is shown for  $T = 1$  mK (staircase) and 100 mK (thick solid curve) as well as for the corresponding classical Heisenberg model at  $T = 0$  (dashed curve). R.h.s.: The thin curve displays the magnetisation following from (4) for  $T = 4$  K. Experimental data using a pulsed field are given by the solid squares, their size reflects an uncertainty of  $\pm 0.5$  T for the data. The thick curve is gives the result of the improved approximation (5), also at 4 K, and closely reproduces the measured values.

In the left panel of Fig. 2 we provide a graph of  $\mathcal{M}/(g\mu_B)$  versus  $B$  as predicted by the quantum model for  $T = 1$  mK (staircase) and 100 mK (thick solid curve), as well as the rigorous result for the corresponding classical Heisenberg model at  $T = 0$ , a strictly linear dependence of  $\mathcal{M}$  on  $B$  up to  $B_c$  (dashed curve). In fact, for  $T > 50$  mK thermal broadening effects smear out the staircase of the quantum model and, above approximately  $B = 0.5$  T,  $\mathcal{M}$  increases linearly with  $B$ , almost parallel to but somewhat below the classical  $T = 0$  result. It would be extremely interesting to put this prediction of staircase-like behavior below 50 mK to a careful experimental test.

What is currently available are experimental data for  $\mathcal{M}$  versus  $B$  on  $\{\text{Mo}_{72}\text{Fe}_{30}\}$ , see the right panel of Fig. 2, as obtained using a pulsed magnetic field. Due to the rapid introduction of the magnetic field, increasing from 0 to 60 Tesla in approximately 6 ms, we estimate that the effective temperature of the spins was 4 K, even though the nominal cryostat temperature was 0.46 K. Nevertheless, the very good agreement between theory and experiment confirms the underlying picture of rotational bands on which the model is based. For a non-parabolic dependence of the energy eigenvalues on  $S$  the magnetisation curve would show unequal steps at  $T = 0$  as well as nonlinear behaviour at higher temperatures. As remarked above, the classical coefficient  $D = D(N, \infty)$  always underestimates the true coefficient  $D(N, s)$  by a few percent [6]. Of course, there is no simple method for establishing the correct value of  $D(30, 5/2)$ , so it is of interest to estimate its value by using the currently available experimental data for  $\mathcal{M}$  versus  $B$ . We attempt to improve approximation (4) quantitatively while ensuring that the rotational band structure is not altered. We adjust  $D(N, s)$  so that the resulting magnetisation curve (thick curve in Fig. 2, r.h.s.) provides an optimal fit to the measured

data. This is achieved by taking  $D(N, s) = 6.23$ , which is very close to  $D = 6$ . Thus an alternate effective Hamiltonian is given by

$$\tilde{H}_2^{\text{eff}} = -J \frac{D(N, s)}{N} \left[ \tilde{S}^2 - \gamma \left( \tilde{S}_A^2 + \tilde{S}_B^2 + \tilde{S}_C^2 \right) \right], \quad (5)$$

with  $\gamma = 1.07$  in order to maintain the correct value of the largest energy eigenvalue. Using (5) we find that  $B_c \approx 18.4$  T. Finally, using this tentative estimate for  $D(30, 5/2)$  enables us to predict the ground state energy of  $\{\text{Mo}_{72}\text{Fe}_{30}\}$  as  $E_0/k_B \approx -339$  K. Taking into account the error bars of the measured data we estimate that the resulting uncertainty of  $D(30, 5/2)$ ,  $\gamma$ , and  $E_0$  is less than 3 %. We are currently attempting to calculate  $D(30, 5/2)$  from first principles using DMRG techniques [13].

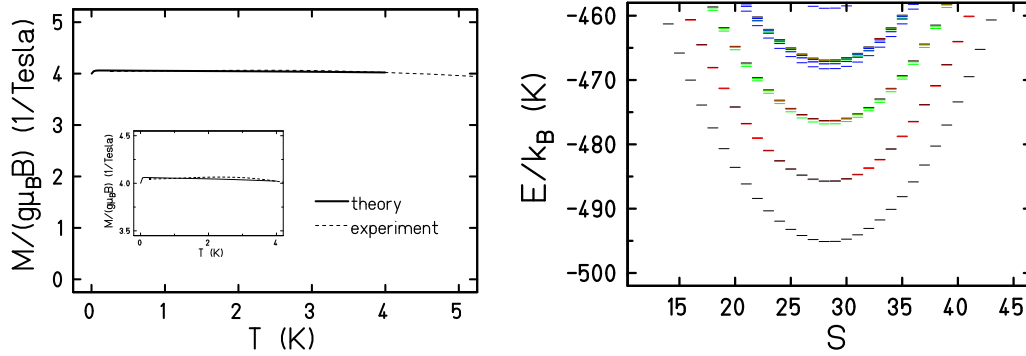


Fig. 3 – L.h.s.: Magnetisation vs. temperature using the four lowest bands of the improved approximate Hamiltonian (5) with  $B = 7.0$  T (solid line); experimental data (dashed line). The near constancy of  $\mathcal{M}$  with  $T$  provides strong evidence that the lowest rotational bands are indeed parabolic. R.h.s.: Low-lying energy eigenvalues in the range shown using  $\tilde{H}_2^{\text{eff}}$  with  $B = 7$  T.

We now compare our theoretical results using (5) and a Zeeman term to our magnetisation measurements at fixed magnetic fields. For both measured field strengths  $B = 5.5$  T (not shown) and  $B = 7.0$  T (Fig. 3, l.h.s.) we find good agreement to the experimental data. The seemingly unexciting result, that both the experimental and theoretical magnetisation  $\mathcal{M}$  are virtually constant over a wide temperature range, actually provides important, indirect confirmation of the existence of a sequence of rotational bands. This can well be understood with the help of the spectrum of  $\tilde{H}_2^{\text{eff}}$  shown in Fig. 3 (r.h.s.) for a finite magnetic field. The levels of the lowest parabola in Fig. 3 (r.h.s.) originate from the  $M = -S$  levels of the lowest rotational band for  $B = 0$  (Fig. 1). Those of the second parabola in Fig. 3 (r.h.s.) originate from the  $M = -S + 1$  levels of the lowest rotational band as well as the  $M = -S$  levels of the second rotational band. Note that the levels of the parabolas are distributed in a very symmetrical manner about their common minimizing value of  $S$  for the given  $B$ . Therefore these levels are populated symmetrically and this leads to a magnetisation which is nearly temperature independent. A slight temperature dependence for  $T \gtrsim 2$  K (see inset of Fig. 3, l.h.s.) stems from small differences in the degeneracies of the individual levels as well as from the fact that the approximate spectrum deviates from the exact one for higher excitation energies. Nevertheless, the near constancy of  $\mathcal{M}$  with  $T$  is therefore also strong evidence that not only the lowest rotational band (3), but also the second is parabolic, for otherwise the symmetry would be broken and  $\mathcal{M}$  would vary significantly with  $T$ .

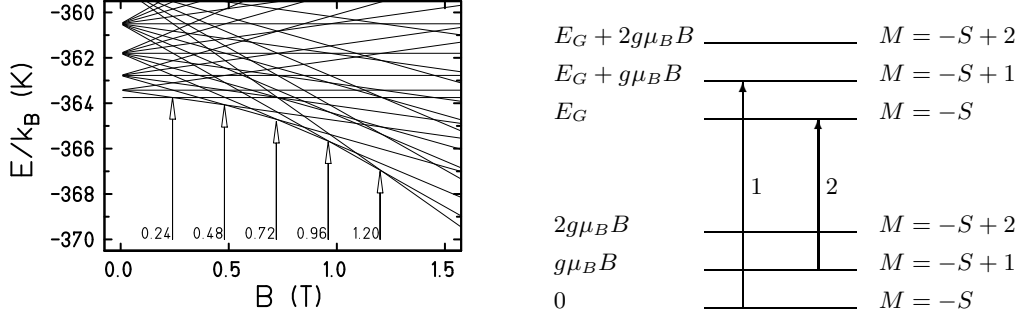


Fig. 4 – L.h.s.: Energy levels of the lowest rotational band as functions of magnetic field. R.h.s. Low-temperature transitions, labelled 1 and 2, which will give rise to peaks in an EPR spectrum involving the lowest Zeeman levels of the two lowest rotational bands, separated by an energy gap  $E_G$ . The gap size  $E_G$  is independent of  $S$ , because the rotational bands are parallel.

The existence of rotational bands implies also the occurrence of resonances of the spin-lattice relaxation rate at low temperatures [14]. Proton NMR probes whether two levels are separated by  $\hbar\omega_L^p$  where  $\omega_L^p$  is the proton Larmor frequency. Since this energy is small compared to the spacings between successive levels of the rotational band in the absence of a magnetic field, resonances of the relaxation rate could be seen close to level crossings induced by the static magnetic field [14]. In the absence of a crystal field the level crossings will be observable at the magnetic fields highlighted in the left panel Fig. 4. The zero-field level spacings of the lowest rotational band are  $\Delta_S = 2(S+1) \cdot 0.16$  K, and thus it will be necessary to go to very low temperatures in order to observe distinct resonance peaks.

We now discuss some of the other consequences of the existence of a sequence of rotational bands. Using Eqs. (4) or (5) we estimate that the gap between the lowest two rotational bands is  $\Delta \approx 8$  K. Inelastic neutron scattering and EPR techniques should provide useful tests of this prediction. In the standard EPR setup, working with a fixed resonance frequency,  $\nu_0$ , and an applied field of variable strength  $B$ , because of the selection rule  $\Delta S = 0$  one can focus on the Zeeman levels of the lowest two rotational bands for a fixed value of  $S$ . In the right panel of Fig. 4 we illustrate two distinct cases where the resonance condition is met for a given value of  $B$ . The arrow marked 1 applies for a case where the inequality  $\nu_G < \nu_0 < 2\nu_G$  is satisfied, where  $\nu_G = E_G/h$  is the gap frequency associated with successive rotational bands. When the resonance condition  $h\nu_0 = E_G + g\mu_B B$  is met (independent of  $S$ ) the additional selection rule  $\Delta M = \pm 1$  allows for a transition from the  $M = -S$  level of the lowest rotational band to the  $M = -S + 1$  level of the first excited rotational band. For the arrow marked 2, which illustrates the case  $\nu_0 < \nu_G$ , the resonance condition reads  $h\nu_0 = E_G - g\mu_B B$ , and it is associated with a transition from the  $M = -S + 1$  level of the lowest rotational band to the  $M = -S$  level of the first excited rotational band. The intensity of the peak will be temperature dependent, proportional to the Boltzmann factor  $\exp(-\beta g\mu_B B)$ .

Anticipating that the Debye temperature of  $\{\text{Mo}_{72}\text{Fe}_{30}\}$  is of order 200–300 K, we believe that specific heat measurements in the temperature range below 0.75 K can serve as a useful

probe of the levels of the lowest rotational band. A comparison between our theory predictions and specific heat data will be given elsewhere [15].

*Summary.* – In summary, in this Letter we have presented an approximate quantum model enabling us to determine the low-temperature properties of the molecular magnet  $\{\text{Mo}_{72}\text{Fe}_{30}\}$ . Several of our results have been confirmed by our measurements and others remain to be tested. The form of the effective Hamiltonian, Eqs. (4) or (5), is set by incorporating the symmetry properties of the spin array which leads to an identification of interacting sublattice spin vectors. Some features of the model (e.g., parallel rotational bands also for high-lying states) are oversimplified, however, these do not play any role on results shown here. The present method, which is based on the notion of parallel rotational excitation bands, offers an insightful and quantitatively useful platform as an alternative to the insurmountable difficulties in treating the exact quantum Heisenberg model. Adaptation of this methodology to still larger, high-symmetry magnetic molecules that will be synthesized in the future can be expected to provide similar benefits.

\* \* \*

We thank A. Müller (Bielefeld) and members of his group, especially P. Kögerler, both for providing us with samples of  $\{\text{Mo}_{72}\text{Fe}_{30}\}$  as well as helpful discussions. We also thank F. Borsa, S. Bud'ko, P. Canfield, M. Exler, H.-J. Schmidt, C. Schröder, and J. Shinar for many helpful discussions. Finally we thank the National Science Foundation and the Deutscher Akademischer Austauschdienst for supporting a mutual exchange program. The Ames Laboratory is operated for the United States Department of Energy by Iowa State University under Contract No. W-7405-Eng-82.

## REFERENCES

- [1] GATTESCHI D. *et al.*, *Science*, **265** (1994) 1054; GATTESCHI D., *Adv. Mater.*, **6** (1994) 635.
- [2] FRIEDMAN J.R. *et al.*, *Phys. Rev. Lett.*, **76** (1996) 3830; THOMAS L. *et al.*, *Nature (London)*, **383** (1996) 145.
- [3] DEARDEN A.L. *et al.*, *Angew. Chem. Int. Ed.*, **40** (2001) 151.
- [4] MÜLLER A. *et al.*, *Angew. Chem. Int. Ed. Engl.*, **38** (1999) 3238; the complete chemical formula of the compound is  $[\text{Mo}_{72}\text{Fe}_{30}\text{O}_{252}(\text{Mo}_2\text{O}_7(\text{H}_2\text{O}))_2(\text{Mo}_2\text{O}_8\text{H}_2(\text{H}_2\text{O}))(\text{CH}_3\text{COO})_{12}(\text{H}_2\text{O})_{91}]\bullet 150\text{H}_2\text{O}$ .
- [5] MÜLLER A. *et al.*, *Solid State Sciences*, **2** (2000) 847.
- [6] SCHNACK J. and LUBAN M., *Phys. Rev. B*, **63** (2001) 014418.
- [7] BERNU B. *et al.*, *Phys. Rev. B*, **50** (1994) 10048.
- [8] AXENOVICH M. and LUBAN M., *Phys. Rev. B*, **63** (2001) 100407.
- [9] CANESCHI A. *et al.*, *Chem. Eur. J.*, **2** (1996) 1379.
- [10] ABBATI G.L. *et al.*, *Inorg. Chim. Acta*, **297** (2000) 291.
- [11] HENLEY C.L. and NAI-GONG ZHANG, *Phys. Rev. Lett.*, **81** (1998) 5221.
- [12] MÜLLER A. *et al.*, *ChemPhysChem*, **2** (2001) 517.
- [13] WHITE S.R., *Phys. Rev. B*, **48** (1993) 10345.
- [14] JULIEN M.-H. *et al.*, *Phys. Rev. Lett.*, **83** (1999) 227.
- [15] BUD'KO S. *et al.*, (in preparation).